Manuscript submitted to
AIMS' Journals
Volume **X**, Number **0X**, XX **200X**

doi:10.3934/xx.xx.xx.xx

pp. **X–XX**

COPS ON THE DOTS IN A MATHEMATICAL MODEL OF URBAN CRIME AND POLICE RESPONSE

Joseph R. Zipkin

Department of Mathematics
University of California, Los Angeles
Los Angeles, CA 90095, USA

Martin B. Short

School of Mathematics
Georgia Institute of Technology
Atlanta, GA 30332, USA

Andrea L. Bertozzi

Department of Mathematics
University of California, Los Angeles
Los Angeles, CA 90095, USA

(Communicated by the associate editor name)

Abstract. Hotspots of crime localized in space and time are well documented. Previous mathematical models of urban crime have exhibited these hotspots but considered a static or otherwise suboptimal police response to them. We introduce a program of police response to hotspots of crime in which the police adapt dynamically to changing crime patterns. In particular, they choose their deployment to solve an optimal control problem at every time. This gives rise to a free boundary problem for the police deployment's spatial support. We present an efficient algorithm for solving this problem numerically and show that police presence can prompt surprising interactions among adjacent hotspots.

1. Introduction.

1.1. **Crime patterns.** Urban crime is ubiquitous and heterogeneous: while it can certainly affect a whole city, clusters of crimes are often localized in time and space, forming "hot spots" of increased criminal activity [5, 9]. Simple spatial heterogeneity in the environment is insufficient to explain the temporal variations in crime recurrence [21]. Rather, the emergence of hot spots is linked to *repeat victimization*: a successful offender likely to re-offend in the same location, or nearby (*near-repeat victimization*). Such patterns have been observed in illicit activities

2010 *Mathematics Subject Classification.* Primary: 35K57, 49M29, 65K10; Secondary: 65M06.

Key words and phrases. Reaction-diffusion equations, optimal control, free boundary problem, crime modeling.

This work was supported by NSF grants DMS-0907931 and DMS-0968309 and by the Army Research Office through ARO MURI grants W911NF-11-1-0332 and W911NF-10-1-0472. The first author is supported by the Department of Defense through the National Defense Science and Engineering Graduate Fellowship program.

from residential burglary [11] to insurgent activity in Iraq [23]. For law enforcement, a seemingly obvious response to a hot spot of crime is to deploy additional resources to the hot spot to deter further crime. These so-called "cops on the dots" strategies have sometimes successfully dispersed the hot spot, but other times have merely displaced the crime to surrounding areas [4].

1.2. **The discrete Short model.** Short et al. [19] introduce an agent-based model for dynamics of crime. Agents are criminals taking a biased random walk on a rectangular lattice with periodic boundary conditions. Time steps are discrete, with length dt. In each time step, each agent either strikes (i.e., commits a crime) at its present node or moves to an adjacent node. The agents' decisions are influenced by a scalar *attractiveness* field A, whose dynamics are coupled to the agents' dynamics.

During time step t, an agent at node x strikes at x with probability

$$p_s(x,t) = 1 - e^{-A(x,t)dt}. \tag{1}$$

Agents who strike exit the system; otherwise they move to an adjacent node. If x' is adjacent to x (denoted hereafter by $x' \sim x$), an agent moves from x to x' with probability $p_m(x,t;x')$, which is proportional to $A(x',t)$.

The attractiveness A is split into a static component A_0 and a dynamic component B so that $A = A_0 + B$. To model repeat victimization, B at x is increased by θ for each strike that occurred at x during the previous time period. Then, to model near-repeat victimization, B diffuses to adjacent nodes and decays. If $S(x,t)$ denotes the number of strikes at node x at time t, the dynamics of B are given by

$$B(x,t+dt) = \left((1-\eta)B(x,t) + \frac{\eta}{4}\sum_{x'\sim x} B(x',t)\right)(1-\omega dt) + \theta S(x,t), \tag{2}$$

where η is a positive parameter.

Let $n(x,t)$ be the number of criminals at node x at time t. In addition to the above movement and exit rules, criminals generate at each node according to a Poisson process with parameter Γ:

$$E(n(x,t+dt)|n(\cdot,t)) = \sum_{x'\sim x} n(x',t)(1-p_s(x,t))p_m(x,t;x') + \Gamma dt, \tag{3}$$

where E denotes the expectation.

Under different choices of parameters, the system can give rise to different hot spot patterns. One such pattern is shown in Fig. 1. The system is in homogeneous equilibrium when all nodes have the same attractiveness $\overline{A} = A_0 + \overline{B}$ and the same average number of criminals $\overline{n}$. The equilibrium values can be found algebraically:

$$\overline{B} = \frac{\theta\Gamma}{\omega}, \qquad\qquad \overline{n} = \frac{\Gamma dt}{1 - e^{\overline{A}dt}}.$$

1.3. **The continuous Short model.** If ℓ is the length between any two grid nodes, then $\rho = E(n)/\ell^2$ is the expectation value of the criminal density. Taking a hydrodynamic limit of (2-3) holding ℓ^2/dt constant as ℓ, $dt \to 0$ (and changing variables to eliminate some parameters) gives a parabolic PDE system:

$$\frac{\partial A}{\partial t} = \eta\triangle A + \rho A - A + A_0 \tag{4}$$

$$\frac{\partial \rho}{\partial t} = \nabla\cdot(\nabla\rho - 2\rho\nabla\log A) - \rho A + \overline{B}. \tag{5}$$

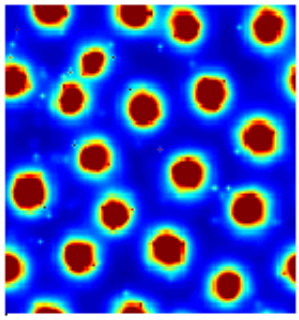

FIGURE 1. A snapshot of the attractiveness A from simulations of the discrete model on a toroidal grid.

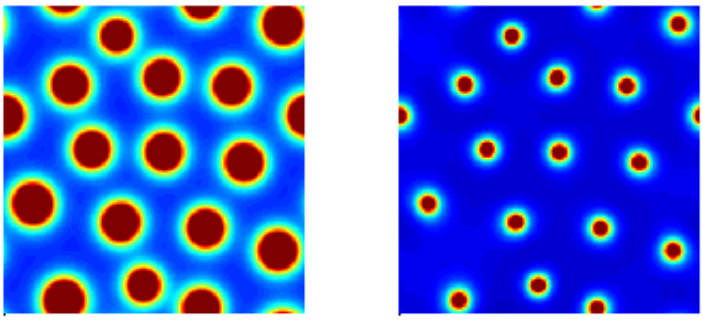

FIGURE 2. A numerical solution of the continuous model (4) (left) and (5) (right) with periodic boundary conditions. $\eta = 0.03$, $A_0 = 0.5$, $\overline{B} = 2.5$.

(The change of variables replaces some parameters with $\overline{B}$, which becomes a parameter together with η and A_0.) This reaction-diffusion system resembles the well known Keller-Segel model of chemotaxis [13, 14, 10]. Rodríguez and Bertozzi [18] demonstrate local existence and uniqueness of solutions for the system; Rodríguez [17] extends this result. Cantrell, Cosner, and Manásevich [7] prove several bifurcation results. Chaturapruek et al. [8] recast both the discrete and continuous short models using Lévy flights to drive the criminals' motion, resulting in a nonlocal PDE system.

Solutions of the PDE system (4-5) exhibit stationary hotspots given appropriate parameters and initial conditions. Fig. 2 shows a typical configuration of attractiveness A (left) and criminal density ρ (right). The solution was computed numerically using techniques described in [19] from a randomly perturbed initial condition. In a steady state solution the configuration of hot spots would be more uniform; however, the convergence from the situation in Fig. 2 to steady state happens over a much longer time scale than the emergence of the hot spots.

Short et al. [19] perform a linear stability analysis and predict what combinations of the parameters $(\eta, A_0, \overline{B})$ will produce the hotspot-generating instability. Instability around the homogeneous steady-state solution $(A, \rho) = (\overline{A}, \overline{\rho})$ has the necessary condition $\overline{B} > \frac{1}{2}A_0$. Once that is satisfied, a sufficient condition is

$$\eta < \frac{3\overline{\rho} + 1 - \sqrt{12\overline{\rho}}}{\overline{B} + A_0}.$$

In the hydrodynamic limit, the expected number of crimes per unit area per unit time follows

$$E\left(\frac{S(x,t)}{\ell^2 dt}\right) \approx \frac{E(n(x,t))}{\ell^2}\frac{p_s(x,t)}{dt} = \rho(x,t)\frac{A(x,t)dt + O(dt^2)}{dt} \to \rho(x,t)A(x,t).$$

The approximation notation $\approx$ is necessary because, as Jones, Brantingham, and Chayes [12] point out, n and p_s are random variables that are likely not independent, but their correlations are not very important for understanding the system's overall dynamics. We will therefore use ρA as a proxy for the amount of crime.

1.4. **Police in the Short model.** The original Short model does not consider police explicitly. In particular, it does not contemplate how criminals would respond to police presence or how police would respond to the emergence of hotspots. Here we review several attempts to answer this question.

In [21] and [20], Short et al. add a deterrence term d to (4-5) to model the effect of police deployment. Deterrence decreases the total crime committed and discourages new criminals from entering the system. The continuum equations become

$$\frac{\partial A}{\partial t} = \eta\triangle A + d\rho A - A + A_0 \tag{6}$$

$$\frac{\partial \rho}{\partial t} = \nabla\cdot(\nabla\rho - 2\rho\nabla\log A) - d\rho A + d\overline{B}. \tag{7}$$

To model a cops-on-the-dots deployment, d is a function of space whose effect is centered at the center of a hotspot. Specifically, if the police start at time t_0, then

$$d(x) = \tfrac{1}{2}\big(1 - \tanh[\mu(A(x,t_0) - A_c)]\big),$$

where μ and A_c are positive parameters. Note that d is not a function of time; it is a fixed deterrence profile based on the attractiveness at time t_0. In [21] and [20] it is shown that the deterrence can dissipate or merely displace hotspots of crime.

Pitcher [16] modifies the original Short model to reflect slightly different assumptions about criminal behavior. Under certain parameters her model is linearly unstable and exhibits numerical solutions with hotspots resembling those in Fig. 2. She also considers the effect of police deploying to minimize crime and facing a resource constraint. Over time the police displace the criminals and the attractiveness to the hotspots' edges, creating ring-like structures.

Jones, Brantingham and Chayes [12] return to the discrete model. They assign their police three deployment strategies: random patrols, in which police take a true random walk through the domain; cops on the dots, in which police, like criminals, take a biased random walk toward areas of greater attractiveness; and peripheral interdiction, in which police are biased to seek out the edges of hot spots. In agreement with research using field data, they find that random patrols are largely ineffective. Cops on the dots is effective early into its implementation, but peripheral interdiction eventually does just as well. For larger hotspots, peripheral interdiction is eventually better at reducing crime than cops on the dots.

1.5. **Other models.** Berestycki and Nadal [1] postulate a different PDE model grounded in economic rather than anthropological literature. Unlike the Short model it is not agent-based, but like the Short model it reflects repeat victimization and exhibits hot spots. Police interact with the system by exerting limited control over the local cost of illegal activity. Given enough resources, an appropriate police strategy can moderate the strength of the hot spots over time. Berestycki, Rodríguez and Ryzhik [2] find traveling wave solutions to the system.

Birks, Townsley, and Stewart [3] present a novel agent-based model of criminal behavior. As in the discrete Short model, criminal agents move through a rectangular grid and decide whether to strike based in part on different levels of attractiveness encountered throughout the domain. However, in their model targets are distributed randomly throughout the domain, rather than uniformly at one per node. Furthermore, agents are constrained to move along nodes of a transport network, also determined randomly. They are more likely to strike at targets near their current position if those targets are more attractive and if they are more aware of the targets. The study finds that hot spots are more likely to emerge if each agent has only a few destination transit nodes, if attractiveness is heterogeneous, and if awareness is heterogeneous. They do not discuss police directly.

2. Optimal deployment of police.

We propose a new method for police deployment that takes into account police departments' ability to strategize and coordinate their motions. Where prior work has postulated either that police deploy to a fixed location or that they may move but without any coordination, we propose that the police are constantly responding to new crimes that are committed. Their rule of movement will be to always deploy to minimize the total crime occurring instantaneously. This approach reflects police's expertise, hierarchy, and coordination, in contrast with criminals who may not collaborate or even share a common goal.

2.1. Model specification.

Return to equations (6-7), but assume now that police need not choose a static deployment based on the state of the system at one point in time. Instead allow them to allocate resources dynamically based on how the system responds to them. Under this framework we need a different understanding of the deterrence factor d. Rather than being a fixed function of space it must change in accordance with how the police choose to deploy. Let $\kappa(x,t)$ be the amount of police resources deployed to point x at time t. Then the deterrence factor prevailing at (x,t) is $d(\kappa(x,t))$, with d now a function from $[0,\infty)$ to $(0,1]$.

Intuition and convenience allow us to describe several properties we expect of d.

Definition 2.1. A function $d:[0,\infty)\to(0,1]$ is a *deterrence function* if and only if each of the following is satisfied:

1. $d(0)=1$: If no police are present at a location, the criminals behave there as they would in the original model.
2. d is decreasing: More police should result in less crime.
3. d is convex: Returns to additional police should diminish.
4. d is C^2: There are no critical levels of police that prevent d from being smooth.
5. d is positive: The police cannot prevent all crime no matter how much they deploy; however,
6. $\lim_{k\to\infty} d(k)=0$: They can achieve a target deterrence level if they deploy enough resources.

Assumptions 3 and 4 together imply by the Inverse Function Theorem that d' is invertible and $(d')^{-1}$ is C^1; we will use this later. The choice $d(k) = e^{-k}$ will be convenient, particularly because of a computational advantage described in section 3.3.

The police deploy to solve a minimization problem. For now we will assume that their goal at time t is to minimize the total crime in the system at time t, that is, $\int d(\kappa)\rho A\,dx$, which we sometimes denote $F(\kappa)$. They face a positivity constraint $\kappa \geq 0$ and some appropriate constraint on their total resources. For now we will assume that at each time step the police must deploy a fixed amount of resources K; that is, for all t, $\int \kappa\,dx = K$.

The problem with dynamic police is therefore

$$\frac{\partial A}{\partial t} = \eta\triangle A + d(\kappa)\rho A - A + A_0, \tag{8}$$

$$\frac{\partial \rho}{\partial t} = \nabla\cdot(\nabla\rho - 2\rho\nabla\log A) - d(\kappa)\rho A + d(\kappa)\overline{B}, \tag{9}$$

$$\kappa = \arg\min\left\{\int_\Omega d(k)\rho A\,dx : k\in L^1(\Omega), k\geq 0, \int_\Omega k\,dx = K\right\}. \tag{10}$$

The optimization problem (10) is the novel part of the model.

The feasible set $\{k \in L^1(\Omega) : k \geq 0, \int_\Omega k\,dx = K\}$ is a convex subset of L^1, and (by the convexity of d) the objective functional $\kappa \mapsto \int d(\kappa)\rho A\,dx$ is a convex functional. Thus the optimization problem is convex. In the dual formulation it becomes a free boundary problem, with the boundary determined by ρ, A, and λ, the dual variable associated to the L^1 constraint.

2.2. **Dual formulation: a free boundary problem.** The dual formulation has an immediate interpretation in the perspective of the police commander deciding where to deploy resources. Each incremental resource should go to the place where it can have the most incremental impact, until all the resources are used up. Limitations on the commander's resources force him to ignore areas where the amount of crime is below some critical threshold. This threshold is determined by the dual variable λ.

Throughout this section, fix t and consider the problem of recovering the optimal κ from ρA. We will assume that the introduction of police into the Short model has not disrupted the continuity guaranteed by [18] too much. In particular, we assume that ρA is continuous.

Theorem 2.2. *Let ρA be non-negative everywhere, positive on a set of positive measure, and continuous. Then there exists $\lambda > 0$ such that*

$$\kappa = (d')^{-1}(-\lambda/\rho A)\chi_{U(\lambda,\rho A)}, \tag{11}$$

where $U(\lambda, f) = \{x \in \Omega : f(x) > -\lambda/d'(0)\}$. This λ is the Lagrange multiplier associated to the L^1 constraint (10) and as such is the unique solution to the nonlinear equation

$$G(\lambda) := \int_{U(\lambda,\rho A)} (d')^{-1}(-\lambda/\rho A)dx = K. \tag{12}$$

The proof of Theorem 2.2 is presented in Lemmas 2.3-2.6. First we dispatch the easy case when $\kappa > 0$ throughout Ω.

Lemma 2.3. *Theorem 2.2 holds if $\kappa > 0$ everywhere.*

Proof. We need not impose the $\kappa \geq 0$ constraint explicitly. Only the L^1 constraint remains, and the Lagrange multiplier method in calculus of variations suffices. The stationarity criterion is $d'(\kappa)\rho A + \lambda = 0$, where λ is the Lagrange multiplier associated to the L^1 constraint. As noted previously d' is invertible, so solving for κ gives (11). Substituting this into the L^1 constraint gives (12), noting that $U(\lambda, \rho A) = \Omega$ in this case.

G is strictly decreasing because d' (and hence $(d')^{-1}$) is strictly increasing. Thus the λ solving (12) is unique. □

Now assume that $\kappa = 0$ on a subset of Ω of positive measure. There exists a Lagrange multiplier $\lambda > 0$ such that $d'(\kappa)\rho A + \lambda = 0$ wherever $\kappa > 0$. The κ defined in (11) is a weakly increasing function of ρA. In particular, there is some threshold value C such that $\kappa(x) > 0$ if $\rho(x)A(x) > C$ but $\kappa(x) = 0$ if $\rho(x)A(x) < C$. Lemmas 2.4 and 2.5 show that $C = -\lambda/d'(0)$. The central idea is that the choice of λ in (12) allows κ to be continuous as ρA passes the $-\lambda/d'(0)$ threshold. Were it not continuous, it would be advantageous to redistribute some κ from the edges of its support to nearby areas where it is 0. Lemma 2.6 proves that this is the unique λ solving (12) by showing that G is strictly decreasing.

Lemma 2.4. $C \geq -\lambda/d'(0)$.

Proof. Suppose otherwise; then $C < -\lambda/d'(0)$. Let $\rho(x)A(x) = \frac{1}{2}(C - \lambda/d'(0))$; such an x exists because ρA is continuous. Then $\kappa(x) > 0$, and

$$d'(\kappa(x)) = -\frac{2\lambda}{C - \lambda/d'(0)}.$$

Both sides are negative, so

$$d'(\kappa(x)) < -\frac{2\lambda}{-\lambda/d'(0) - \lambda/d'(0)} = d'(0).$$

But by assumption d is convex, so $d'(\kappa(x)) > d'(0)$. Thus $C \geq -\lambda/d'(0)$. □

Lemma 2.5. $C \leq -\lambda/d'(0)$.

Proof. Suppose otherwise; then $C > -\lambda/d'(0)$. Let $\epsilon \in (0, \frac{1}{2}C)$. Because ρA is continuous, there exist $\delta > 0$ and open subsets U^+, U^- of Ω such that $|U^+| = |U^-| = \delta$, $0 < \rho A - C < \epsilon$ in U^+, and $0 < C - \rho A < \epsilon$ in U^-. By definition of C, κ is positive in U^+ but zero in U^-. In particular, letting $\kappa^* = (d')^{-1}(-\lambda/C)$ $\kappa > \kappa^* > 0$ in U^+. This last set of inequalities is independent of ϵ, so we are free to further stipulate that $\epsilon < \frac{1}{2}\kappa^*$.

Now let $\hat{\kappa} = \kappa - \epsilon\chi_{U^+} + \epsilon\chi_{U^-}$, where χ_V is the indicator function on the set V. This $\hat{\kappa}$ meets the positivity and L^1 constraints, and

$$\begin{aligned}
F(\hat{\kappa}) - F(\kappa) &= \int_{U^+} (d(\kappa - \epsilon) - d(\kappa))\rho A\, dx + \int_{U^-} (d(\kappa + \epsilon) - d(\kappa))\rho A\, dx \\
&= \int_{U^+} (d(\kappa - \epsilon) - d(\kappa))\rho A\, dx + \int_{U^-} (d(\epsilon) - 1)\rho A\, dx \\
&< \int_{U^+} (d(\kappa - \epsilon) - d(\kappa))(C + \epsilon) dx + \int_{U^-} (d(\epsilon) - 1)(C - \epsilon) dx \\
&= (C + \epsilon) \int_{U^+} (d(\kappa - \epsilon) - d(\kappa)) dx + \delta(C - \epsilon)(d(\epsilon) - 1). \qquad (13)
\end{aligned}$$

By Taylor's theorem, there exists $\epsilon^*(0) \in (0,\epsilon)$ such that $d(\epsilon) - 1 = d'(0)\epsilon + \frac{1}{2}d''(\epsilon^*(0))\epsilon^2$. Let M be the supremum of all values of $d''(k)$ such that k is within $\frac{1}{2}\kappa^*$ of any value taken by κ. M is finite because Ω is finite, κ is finite, and d'' is continuous. M is positive because d'' is positive. We can therefore write

$$d(\epsilon) - 1 \leq d'(0)\epsilon + \tfrac{1}{2}M\epsilon^2. \tag{14}$$

By similar reasoning, for each κ there exists $\epsilon^*(\kappa) \in (0,\epsilon)$ such that

$$d(\kappa - \epsilon) - d(\kappa) = -d'(\kappa)\epsilon + \tfrac{1}{2}d''(\kappa - \epsilon^*(\kappa))\epsilon^2 \leq -d'(\kappa)\epsilon + \tfrac{1}{2}M\epsilon^2. \tag{15}$$

Substituting (14) and (15) into (13),

$$\begin{aligned}
F(\hat{\kappa}) - F(\kappa) &< (C+\epsilon)\int_{U^+} \big(-d'(\kappa)\epsilon + \tfrac{1}{2}M\epsilon^2\big)dx + \delta(C-\epsilon)\big(d'(0)\epsilon + \tfrac{1}{2}M\epsilon^2\big) \\
&= -(C+\epsilon)\epsilon\int_{U^+} d'(\kappa)dx + \delta(C-\epsilon)d'(0)\epsilon + \delta CM\epsilon^2 \\
&< -(C+\epsilon)\epsilon\int_{U^+} d'(\kappa^*)dx + \delta(C-\epsilon)d'(0)\epsilon + \delta CM\epsilon^2 \\
&= -\delta(C+\epsilon)d'(\kappa^*)\epsilon + \delta(C-\epsilon)d'(0)\epsilon + \delta CM\epsilon^2 \\
&= \delta C(d'(0) - d'(\kappa^*))\epsilon + \delta(CM - d'(\kappa^*) - d'(0))\epsilon^2.
\end{aligned}$$

Choose ϵ small enough that the first-order term dominates. Because d' is increasing, this term is negative. Thus $F(\hat{\kappa}) - F(\kappa) < 0$, but then κ is not optimal. Thus $C \leq -\lambda/d'(0)$. □

Therefore, as predicted, $C = -\lambda/d'(0)$, implying (11). This in turn implies (12), so it remains only to show that λ solves (12) uniquely. Lemma 2.6 suffices for this.

Lemma 2.6. *G is strictly decreasing.*

Proof. If $h > 0$, then

$$\begin{aligned}
\frac{G(\lambda+h) - G(\lambda)}{h} &= \int_{U(\lambda+h,\rho A)} \frac{(d')^{-1}(-(\lambda+h)/\rho A) - (d')^{-1}(-\lambda/\rho A)}{h}dx \\
&\quad - \frac{1}{h}\int_{U(\lambda,\rho A)\setminus U(\lambda+h,\rho A)} (d')^{-1}(-\lambda/\rho A)dx \\
&=: I_1(h) - I_2(h).
\end{aligned}$$

Because everything is continuous,

$$\lim_{h\to 0^+} I_1(h) = \int_{U(\lambda,\rho A)} \frac{\partial}{\partial\lambda}(d')^{-1}(-\lambda/\rho A)dx = -\int_{U(\lambda,\rho A)} \frac{1}{\rho A d''((d')^{-1}(-\lambda/\rho A))}dx.$$

Because $h > 0$,

$$\begin{aligned}
I_2(h) &< \frac{1}{h}\int_{U(\lambda,\rho A)\setminus U(\lambda+h,\rho A)} (d')^{-1}\left(\frac{-\lambda}{-(\lambda+h)/d'(0)}\right)dx \\
&= \frac{|U(\lambda,\rho A)\setminus U(\lambda+h,\rho A)|}{h}(d')^{-1}\left(\frac{\lambda}{\lambda+h}d'(0)\right).
\end{aligned}$$

The Taylor approximation

$$(d')^{-1}\left(\frac{\lambda}{\lambda+h}d'(0)\right) = -\frac{d'(0)}{\lambda d''(0)}h + o(h)$$

then yields

$$\begin{aligned} I_2(h) &< -\frac{d'(0)}{\lambda d''(0)}|U(\lambda,\rho A)\setminus U(\lambda+h,\rho A)| + o(1) \\ &= -\frac{d'(0)}{\lambda d''(0)}|\{-\lambda/d'(0) < \rho A \le -(\lambda+h)/d'(0)\}| + o(1). \end{aligned}$$

By a standard measure-theoretic argument,

$$\lim_{h\to 0^+} I_2(h) \le -\frac{d'(0)}{\lambda d''(0)}\left|\bigcap_{h>0}\{-\lambda/d'(0) < \rho A \le -(\lambda+h)/d'(0)\}\right| = 0.$$

But $I_2(h) > 0$ by definition, so

$$\lim_{h\to 0^+} I_2(h) = 0.$$

Thus

$$\lim_{h\to 0^+}\frac{G(\lambda+h)-G(\lambda)}{h} = -\int_{\{\rho A > -\lambda/d'(0)\}}\frac{1}{\rho A d''((d')^{-1}(-\lambda/\rho A))}dx < 0.$$

If $h<0$, then

$$\begin{aligned} \frac{G(\lambda+h)-G(\lambda)}{h} &= \frac{1}{h}\int_{U(\lambda+h,\rho A)\setminus U(\lambda,\rho A)}(d')^{-1}(-(\lambda+h)/\rho A)dx \\ &\quad + \int_{U(\lambda,\rho A)}\frac{(d')^{-1}(-(\lambda+h)/\rho A)-(d')^{-1}(-\lambda/\rho A)}{h}dx \\ &=: I_3(h)+I_4(h). \end{aligned}$$

As before,

$$\lim_{h\to 0^-} I_4(h) = \int_{U(\lambda,\rho A)}\frac{\partial}{\partial\lambda}(d')^{-1}(-\lambda/\rho A)dx = -\int_{U(\lambda,\rho A)}\frac{1}{\rho A d''((d')^{-1}(-\lambda/\rho A))}dx.$$

We cannot guarantee that $\lim_{h\to 0^-} I_3(h) = 0$. This is because

$$\lim_{h\to 0^-}|U(\lambda+h,\rho A)\setminus U(\lambda,\rho A)| = |\{\rho A = -\lambda/d'(0)\}|,$$

which is not necessarily 0. (If it is, then the left- and right-handed derivatives have the same negative value, and we are through.) However, we do have the bounds

$$\frac{d'(0)}{\lambda d''(0)}|\{-(\lambda+h)/d'(0) < \rho A \le -\lambda/d'(0)\}| + o(1) \le I_3(h) \le 0$$

as $h\to 0^-$. Thus the left-handed derivative is no greater than the right-handed derivative, which is itself negative, and G is strictly decreasing. □

We may therefore replace (10) in the statement of the problem with (12), with κ understood to be given explicitly by (11). This formulation will be helpful for determining κ numerically.

Geometrically, λ specifies the threshold crime level below which the police will not bother to deploy. This level is precisely λ scaled by the positive constant $-1/d'(0)$. As the system evolves, λ too will change. Implicit differentiation in t on the equation $G(\lambda) = K$ gives

$$\frac{\lambda_t}{\lambda} = \frac{\int_{U(\lambda,\rho A)}\frac{1}{\rho A d''(\kappa)}(\frac{A_t}{A}+\frac{\rho_t}{\rho})dx}{\int_{U(\lambda,\rho A)}\frac{1}{\rho A d''(\kappa)}dx}.$$

Thus the growth rate of λ is determined by a weighted average of the growth rates of A and ρ inside $U(\lambda, \rho A)$, the region in which the police are deployed. In particular, if ρ and A reach steady state inside $U(\lambda, \rho A)$, then $\lambda_t = 0$, and the whole system is in steady state.

Corollary 2.7 reveals why exponential deterrence will be so convenient later on.

Corollary 2.7. *If $d(k) = e^{-k}$, then throughout $U(\lambda, \rho A)$, $d(\kappa)\rho A = \lambda$.*

Proof. A straightforward calculation following from $(d')^{-1}(y) = -\log(-y)$. □

2.3. **Linear stability.** The homogeneous steady state solution $(A, \rho, \kappa) = (\tilde{A}, \tilde{\rho}, \tilde{\kappa})$ to (8-10) is given by

$$\tilde{A} = d(\tilde{\kappa})\overline{B} + A_0, \qquad \tilde{\rho} = \frac{\overline{B}}{\tilde{A}}, \qquad \tilde{\kappa} = \frac{K}{|\Omega|}. \tag{16}$$

We can also write $\tilde{A} = d(\tilde{\kappa})\overline{A} + (1 - d(\tilde{\kappa}))A_0$. The equilibrium value of A is thus a convex combination of the equilibrium value without police ($\overline{A}$) and its minimum possible value (A_0). More police decreases $\tilde{A}$ but increases $\tilde{\rho}$ proportionally, so that $\tilde{\rho}\tilde{A} = \overline{\rho}\overline{A}$. The average amount of crime in Ω is $d(\tilde{\kappa})\tilde{\rho}\tilde{A}$, less by a factor of $d(\tilde{\kappa})$ than in the system without police.

To understand how the addition of police impacts the stability of the system, we perform a linear stability analysis centered at this equilibrium. Because κ is completely determined at each time by A and ρ, we perturb only A and ρ and then determine the consequences on κ. Let $\epsilon > 0$ be a small parameter specifying the scale of the perturbation: $A = \tilde{A} + \epsilon a$, $\rho = \tilde{\rho} + \epsilon r$. The scale parameter ϵ relative to the perturbations a and r is such that A and ρ are positive everywhere. Let κ denote the solution to (10) given this A and ρ.

First we prove that, if ϵ is small enough, then $\kappa > 0$ throughout Ω.

Proposition 2.8. *Let $K > 0$, and let ρA be positive and bounded. Then there exists $\epsilon_0 > 0$ such that, if $0 < \epsilon < \epsilon_0$, then κ as defined in (10) is positive throughout Ω.*

Proof. It suffices to show that, for all $y \in \Omega$,

$$\int_\Omega (d')^{-1}\left(d'(0)\frac{\rho(y)A(y)}{\rho(x)A(x)}\right)dx < K.$$

If this is so, then the police deploy to every point in Ω. Let $M = \max(\max|a|, \max|r|)$. Because $(d')^{-1}$ is increasing and $d'(0) < 0$,

$$\begin{aligned}\int_\Omega (d')^{-1}\left(d'(0)\frac{\rho(y)A(y)}{\rho(x)A(x)}\right)dx &\le \int_\Omega (d')^{-1}\left(d'(0)\frac{\min\rho A}{\max\rho A}\right)dx \\ &\le \int_\Omega (d')^{-1}\left(d'(0)\frac{\tilde{\rho}\tilde{A} + (\tilde{\rho}+\tilde{A})M\epsilon + M^2\epsilon^2}{\tilde{\rho}\tilde{A} - (\tilde{\rho}+\tilde{A})M\epsilon - M^2\epsilon^2}\right)dx \\ &= |\Omega|(d')^{-1}\left(d'(0)\frac{\tilde{\rho}\tilde{A} + (\tilde{\rho}+\tilde{A})M\epsilon + M^2\epsilon^2}{\tilde{\rho}\tilde{A} - (\tilde{\rho}+\tilde{A})M\epsilon - M^2\epsilon^2}\right). \end{aligned} \tag{17}$$

When $\epsilon = 0$, the quantity in (17) is 0. It is also a continuous function of ϵ, so it is less than K up to some positive value, say ϵ_0. For $\epsilon \in (0, \epsilon_0)$, $\kappa > 0$ throughout Ω. □

Assuming henceforth that ϵ is small enough to satisfy Proposition 2.8,

$$\kappa = (d')^{-1}\left(-\frac{\lambda(\epsilon)}{(\tilde{\rho}+\epsilon r)(\tilde{A}+\epsilon a)}\right).$$

Note the dependence of λ on ϵ. We seek a Taylor expansion of κ in ϵ, centered at $\epsilon = 0$. By assumption, when $\epsilon = 0$, $\kappa = \tilde{\kappa}$. For the linear coefficient,

$$\begin{aligned}\frac{\partial \kappa}{\partial \epsilon}\Big|_{\epsilon=0} &= \frac{1}{d''\big((d')^{-1}(-\lambda(0)/\tilde{\rho}\tilde{A})\big)} \cdot -\frac{\tilde{\rho}\tilde{A}\lambda'(0) - (\tilde{\rho}a + \tilde{A}r)\lambda(0)}{\tilde{\rho}^2\tilde{A}^2} \\ &= \frac{1}{d''(\tilde{\kappa})}\left(\frac{(\tilde{\rho}a + \tilde{A}r)\lambda(0)}{\tilde{\rho}^2\tilde{A}^2} - \frac{\lambda'(0)}{\tilde{\rho}\tilde{A}}\right). \end{aligned} \tag{18}$$

Recalling that $\lambda(0)$ is the Lagrange multiplier associated to the homogeneous steady state, $\lambda(0) = -d'(\tilde{\kappa})\tilde{\rho}\tilde{A}$. We get $\lambda'(0)$ through implicit differentiation on the L^1 constraint

$$\int_\Omega (d')^{-1}\left(\frac{\lambda(\epsilon)}{(\tilde{\rho} + \epsilon r)(\tilde{A} + \epsilon a)}\right) dx = K.$$

Differentiating with respect to ϵ and setting $\epsilon = 0$,

$$\int_\Omega \frac{1}{d''(\tilde{\kappa})}\left(\frac{(\tilde{\rho}a + \tilde{A}r)\lambda(0)}{\tilde{\rho}^2\tilde{A}^2} - \frac{\lambda'(0)}{\tilde{\rho}\tilde{A}}\right) dx = 0$$

$$\lambda'(0) = \frac{\lambda(0)}{|\Omega|\tilde{\rho}\tilde{A}}\left(\tilde{\rho}\int_\Omega a\,dx + \tilde{A}\int_\Omega r\,dx\right).$$

Assuming the perturbations have zero spatial mean, $\lambda'(0) = 0$. Substituting into (18),

$$\frac{\partial \kappa}{\partial \epsilon}\Big|_{\epsilon=0} = \frac{1}{d''(\tilde{\kappa})}\frac{(\tilde{\rho}a + \tilde{A}r)\cdot -d'(\tilde{\kappa})\tilde{\rho}\tilde{A}}{\tilde{\rho}^2\tilde{A}^2} = -\frac{d'(\tilde{\kappa})}{d''(\tilde{\kappa})}\Big(\frac{r}{\tilde{\rho}} + \frac{a}{\tilde{A}}\Big).$$

Thus

$$\kappa = \tilde{\kappa} - \frac{d'(\tilde{\kappa})}{d''(\tilde{\kappa})}\Big(\frac{r}{\tilde{\rho}} + \frac{a}{\tilde{A}}\Big)\epsilon + o(\epsilon).$$

This leads to an expansion of $d(\kappa)$ about $\epsilon = 0$:

$$d(\kappa) = d(\tilde{\kappa}) - \frac{d'(\tilde{\kappa})^2}{d''(\tilde{\kappa})}\Big(\frac{r}{\tilde{\rho}} + \frac{a}{\tilde{A}}\Big)\epsilon + o(\epsilon).$$

Substitute the perturbation into (8):

$$\begin{aligned}\epsilon\frac{\partial a}{\partial t} &= \epsilon\eta\triangle a + \left(d(\tilde{\kappa}) - \frac{d'(\tilde{\kappa})^2}{d''(\tilde{\kappa})}\Big(\frac{r}{\tilde{\rho}} + \frac{a}{\tilde{A}}\Big)\epsilon\right)(\tilde{A} + \epsilon a)(\tilde{\rho} + \epsilon r) - (\tilde{A} + \epsilon a - A_0) + o(\epsilon) \\ &= d(\tilde{\kappa})\tilde{A}\tilde{\rho} - (\tilde{A} - A_0) \\ &\quad + \left(\eta\triangle a - a + d(\tilde{\kappa})\tilde{A}r + d(\tilde{\kappa})\tilde{\rho}a - \frac{d'(\tilde{\kappa})^2}{d''(\tilde{\kappa})}\tilde{\rho}\tilde{A}\Big(\frac{r}{\tilde{\rho}} + \frac{a}{\tilde{A}}\Big)\right)\epsilon + o(\epsilon).\end{aligned}$$

The order-1 terms cancel by (16). Disregarding the superlinear terms, we get

$$\frac{\partial a}{\partial t} = \eta\triangle a - a + \left(d(\tilde{\kappa}) - \frac{d'(\tilde{\kappa})^2}{d''(\tilde{\kappa})}\right)\tilde{\rho}a + \left(d(\tilde{\kappa}) - \frac{d'(\tilde{\kappa})^2}{d''(\tilde{\kappa})}\right)\tilde{A}r$$

Follow the same course for (9):

$$\frac{\partial r}{\partial t} = \triangle r - d(\tilde{\kappa})\tilde{A}r - \frac{2\tilde{\rho}}{\tilde{A}}\triangle a - d(\tilde{\kappa})\tilde{\rho}a.$$

We choose the form $a(x,t) = r(x,t) = e^{\sigma t + in\cdot x}$ for the perturbations so they will be eigenfunctions of the differential operators $\partial/\partial t$ and $\triangle$. The equations are

radial, so we can let n be scalar: $a(x,t) = r(x,t) = e^{\sigma t + in(x_1+x_2)}$ This yields the eigenvalue system

$$\begin{pmatrix} -\eta n^2 - 1 + D(\tilde{\kappa})\tilde{\rho} & D(\tilde{\kappa})\tilde{A} \\ \frac{2\tilde{\rho}}{\tilde{A}} n^2 - d(\tilde{\kappa})\tilde{\rho} & -n^2 - d(\tilde{\kappa})\tilde{A} \end{pmatrix} \begin{pmatrix} a \\ r \end{pmatrix} = \sigma \begin{pmatrix} a \\ r \end{pmatrix} \tag{19}$$

where $D(\tilde{\kappa}) = d(\tilde{\kappa}) - d'(\tilde{\kappa})^2/d''(\tilde{\kappa})$. Note that $D(\tilde{\kappa}) < d(\tilde{\kappa})$.

This system can be linearly unstable, for example if $\eta = \frac{1}{10}$, $A_0 = \frac{1}{100}$, $\overline{B} = \frac{1}{2}$, $d(\kappa) = (1+\kappa)^{-1}$, $K = 1$, $n = 1$. For the remainder of this section we present sufficient conditions for linear stability (or equivalently necessary conditions for linear instability) because these give clues to how effective police can be in stopping crime. We begin with a special case.

Proposition 2.9. *If d is exponential, then the system is unconditionally linearly stable.*

Proof. In this case D is identically 0. The matrix is triangular, and its unconditionally negative eigenvalues can be read off the diagonal. □

This is a marked contrast with the $K = 0$ case, the original Short system, in which the proper choice of parameters can yield linear instability [19]; this system is linearly stable for any positive value of K. The key to the discontinuity lies in Proposition 2.8: given $K > 0$, κ is everywhere positive once ϵ is small enough. In contrast, when $K = 0$, κ cannot be positive anywhere.

Of course, $D(\tilde{\kappa})$ need not be identically 0 in general.[1] Theorem 2.11 states that even these scenarios can be stabilized given enough police. It and several other results rely on the following lemma.

Lemma 2.10. *For all η, A_0, $\overline{B}$, $K > 0$ and every deterrence function d, if the system is linearly unstable, then*

$$1 + d(\tilde{\kappa})\eta\tilde{A} - 3D(\tilde{\kappa})\tilde{\rho} < -\eta. \tag{20}$$

Proof. The greater of the eigenvalues of the matrix in (19) is

$$\sigma_n = \frac{-q_n + \sqrt{q_n^2 - 4\big(\eta n^4 + (1 + d(\tilde{\kappa})\eta\tilde{A} - 3D(\tilde{\kappa})\tilde{\rho})n^2 + d(\tilde{\kappa})\tilde{A}\big)}}{2} \tag{21}$$

where $q_n = 1 + d(\tilde{\kappa})\tilde{A} + (1+\eta)n^2 - D(\tilde{\kappa})\tilde{\rho}$. The system is linearly unstable if and only if $\operatorname{Re}\sigma_n > 0$ for some integer n.

First we show that $q_n > 0$, for which $q_0 > 0$ suffices. First,

$$d(\tilde{\kappa})(d(\tilde{\kappa})\overline{B} + A_0)^2 + \overline{B}\frac{d'(\tilde{\kappa})^2}{d''(\tilde{\kappa})} > 0$$

$$d(\tilde{\kappa})\overline{B} + A_0 + d(\tilde{\kappa})(d(\tilde{\kappa})\overline{B} + A_0)^2 - \left(d(\tilde{\kappa}) - \frac{d'(\tilde{\kappa})^2}{d''(\tilde{\kappa})}\right)\overline{B} > A_0$$

$$1 + d(\tilde{\kappa})(d(\tilde{\kappa})\overline{B} + A_0) - \left(d(\tilde{\kappa}) - \frac{d'(\tilde{\kappa})^2}{d''(\tilde{\kappa})}\right)\frac{\overline{B}}{d(\tilde{\kappa})\overline{B} + A_0} > \frac{A_0}{d(\tilde{\kappa})\overline{B} + A_0}.$$

Recalling the definitions of $\tilde{A}$ and $\tilde{\rho}$ from (16),

$$1 + d(\tilde{\kappa})\tilde{A} - D(\tilde{\kappa})\tilde{\rho} > \frac{A_0}{\tilde{A}},$$

[1] Indeed the only deterrence function d solving the differential equation $D(k) = 0$ is $d(k) = e^{-ck}$, with c a constant of integration.

so $q_0 > 0$.

Thus $\operatorname{Re}\sigma_n > 0$ only if the square root in (21) is real and greater than q_n. Equivalently, there exists an integer n such that

$$\eta n^4 + (1 + d(\tilde{\kappa})\eta\tilde{A} - 3D(\tilde{\kappa})\tilde{\rho})n^2 + d(\tilde{\kappa})\tilde{A} < 0. \tag{22}$$

Equivalently, the polynomial f_1 defined by

$$f_1(x) = \eta x^2 + (1 + d(\tilde{\kappa})\eta\tilde{A} - 3D(\tilde{\kappa})\tilde{\rho})x + d(\tilde{\kappa})\tilde{A}$$

has two real roots, and a positive square integer lies between them. This is true only if the greater root of f_1 is greater than 1:

$$\frac{-(1 + d(\tilde{\kappa})\eta\tilde{A} - 3D(\tilde{\kappa})\tilde{\rho}) + \sqrt{(1 + d(\tilde{\kappa})\eta\tilde{A} - 3D(\tilde{\kappa})\tilde{\rho})^2 - 4\eta d(\tilde{\kappa})\tilde{A}}}{2\eta} > 1.$$

Equivalently,

$$\sqrt{(1 + d(\tilde{\kappa})\eta\tilde{A} - 3D(\tilde{\kappa})\tilde{\rho})^2 - 4d(\tilde{\kappa})\eta\tilde{A}} > 2\eta + 1 + d(\tilde{\kappa})\eta\tilde{A} - 3D(\tilde{\kappa})\tilde{\rho}. \tag{23}$$

If the right-hand side of (23) is positive, then we can square both sides, leading ultimately to the inequality

$$1 + d(\tilde{\kappa})\eta\tilde{A} - 3D(\tilde{\kappa})\tilde{\rho} < -\eta - d(\tilde{\kappa})\tilde{A}.$$

If the right-hand side of (23) is negative, then

$$1 + d(\tilde{\kappa})\eta\tilde{A} - 3D(\tilde{\kappa})\tilde{\rho} < -2\eta.$$

In either case, (20) holds. □

Theorem 2.11. *For all η, A_0, $\overline{B} > 0$ and every deterrence function d, there exists $K^* > 0$ such that the system is linearly stable if $K > K^*$.*

Proof. Suppose the system is linearly unstable. Then (20) holds, which implies

$$1 + d(\tilde{\kappa})\eta\tilde{A} - 3d(\tilde{\kappa})\tilde{\rho} < -\eta.$$

Per (16), substitute $\overline{B}/\tilde{A}$ for $\tilde{\rho}$ and $d(\tilde{\kappa})\overline{B} + A_0$ for $\tilde{A}$. Collect terms in $d(\tilde{\kappa})$:

$$\eta\overline{B}^2 d(\tilde{\kappa})^3 + 2\eta A_0\overline{B}d(\tilde{\kappa})^2 + (\eta A_0^2 + (\eta - 2)\overline{B})d(\tilde{\kappa}) + (\eta + 1)A_0 \le 0.$$

Define the polynomial f_2 by

$$f_2(y) = \eta\overline{B}^2 y^3 + 2\eta A_0\overline{B}y^2 + (\eta A_0^2 + (\eta - 2)\overline{B})y + (\eta + 1)A_0.$$

Because $f_2(0) = (\eta + 1)A_0 > 0$, by the intermediate value theorem there exists $y_2 \in (0, 1]$ such that $f_1(y) \ge 0$ for all $y \in [0, y_2]$. Let $K^* = d^{-1}(y_2)|\Omega|$. By Definition 2.1, if $K > K^*$, then $d(\tilde{\kappa}) \le y_2$. Thus $f_2(d(\tilde{\kappa})) \ge 0$, so by Lemma 2.10 the system is linearly stable. □

Thus K^* is bounded from above in terms of the zeros of a cubic polynomial. Specifically, y_2 is the lesser of 1 and the least positive root of f_2, if it has a positive root. If it does not, then the system is linearly stable for all $K > 0$.

The K^* found in the above proof is by no means sharp. Indeed, Proposition 2.9 tells us that $K^* = 0$ when d is exponential. Even in general cases we may be able to sharpen it further. For (22) to hold, the polynomial f_1 must have two real roots, so its discriminant must be positive. Equivalently,

$$(1 + d(\tilde{\kappa})\eta\tilde{A} - 3D(\tilde{\kappa})\tilde{\rho})^2 \ge 4d(\tilde{\kappa})\eta\tilde{A}. \tag{24}$$

If $1 + d(\tilde{\kappa})\eta\tilde{A} - 3D(\tilde{\kappa})\tilde{\rho} > 0$, then the roots of p are not positive, so (24) reduces to

$$1 + d(\tilde{\kappa})\eta\tilde{A} - 3D(\tilde{\kappa})\tilde{\rho} \leq -2\sqrt{d(\tilde{\kappa})\eta\tilde{A}}. \tag{25}$$

If we use (25) in the place of (20) in the proof of Theorem 2.11, we get the function f_3 defined by

$$f_3(y) = \eta\overline{B}^2 y^3 + 2\eta A_0 \overline{B} y^2 + (\eta A_0^2 - 2\overline{B})y + 2\sqrt{\eta}(\overline{B}y + A_0)^{3/2} y^{1/2} + A_0.$$

in the place of f_2. Because f_3 is continuous and $f_3(0) > 0$, a similar intermediate value theorem argument works here as well. If y_3 is the lesser of 1 and the least positive root of f_3, then $K^* = \min(d^{-1}(y_2), d^{-1}(y_3))|\Omega|$. Corollary 2.19 sharpens K^* further.

Moreover, Theorem 2.11 is not the only sufficient condition for linear stability. Propositions 2.12 and 2.14 and Corollaries 2.13 and 2.15 provide conditions relying only on the parameters η, A_0, and $\overline{B}$.

Proposition 2.12. *If $\eta \geq 2\overline{B}/(\overline{B} + A_0^2)$, then the system is linearly stable.*

Proof. The polynomial f_2 has all positive coefficients, except possibly for the linear coefficient. If $\eta \geq 2\overline{B}/(\overline{B} + A_0^2)$, then the linear coefficient is non-negative, so f_2 is monotone. Thus it can have no positive roots, since $f_2(0) > 0$. □

Corollary 2.13. *If $\eta \geq 2$, then the system is linearly stable.*

Proposition 2.14. *If $\eta \geq (2\overline{B} - A_0)/(\overline{B} + A_0)$, then the system is linearly stable.*

Proof. Write (20) as

$$(\eta + 1)A_0 + (\eta - 2)d(\tilde{\kappa})\overline{B} + d(\tilde{\kappa})\eta(d(\tilde{\kappa})\overline{B} + A_0)^2 < -3\overline{B}\frac{d'(\tilde{\kappa})^2}{d''(\tilde{\kappa})}.$$

If the system is linearly unstable, then $\eta - 2 < 0$ by Corollary 2.13. Because the right-hand side is negative and $0 < d(\tilde{\kappa}) < 1$,

$$(\eta + 1)A_0 + (\eta - 2)\overline{B} < 0. \tag{26}$$

Because (20) is necessary for linear instability by Lemma 2.10, so is (26). □

Corollary 2.15. *If $2\overline{B} \leq A_0$, then the system is linearly stable.*

Since stating Theorem 2.11 we have ignored the information about the shape of d encoded in the $d'(\tilde{\kappa})^2/d''(\tilde{\kappa})$ term of $D(\tilde{\kappa})$. We now use it and Lemma 2.10 to treat another special case.

Proposition 2.16. *If $d(\kappa) = (1 + \kappa)^{-p}$ with $p \geq 2$, then the system is linearly stable.*

Proof. In this case,

$$D(\kappa) = \tfrac{1}{p+1}(1 + \kappa)^{-p} = \tfrac{1}{p+1}d(\kappa).$$

Substituting this into (20) gives

$$1 + d(\tilde{\kappa})\eta\tilde{A} - \tfrac{3}{p+1}d(\tilde{\kappa})\tilde{\rho} < -\eta.$$

Collecting terms in $d(\tilde{\kappa})$,

$$\eta\overline{B}^2 d(\tilde{\kappa})^3 + 2\eta A_0\overline{B}d(\tilde{\kappa})^2 + (\eta A_0^2 + (\eta + 1 - \tfrac{3}{p+1})\overline{B})d(\tilde{\kappa}) + (\eta + 1)A_0 < 0.$$

This can hold only if the polynomial f_4 defined by

$$f_4(y) = \eta\overline{B}^2 y^3 + 2\eta A_0\overline{B}y^2 + (\eta A_0^2 + (\eta + 1 - \tfrac{3}{p+1})\overline{B})y + (\eta + 1)A_0$$

has a root between 0 and 1. Since $f_4(0) > 0$ and all coefficients are positive, except perhaps for the linear coefficient, the linear coefficient must be negative for such a root to exist. Thus

$$p < \frac{3}{\eta + 1 + \eta A_0^2/\overline{B}} - 1$$

is a necessary condition for linear stability. But this is impossible if $p \geq 2$. □

Proposition 2.17 uses the $(d')^2/d''$ information to show that, in general, d must decay slower than exponentially in unstable regions.

Proposition 2.17. *Given η, A_0, $\overline{B} > 0$ and a deterrence function d, let $[K_1, K_2]$ be an interval such that the system is linearly unstable if $K_1 \leq K \leq K_2$. If $K_1 < K \leq K_2$, then*

$$d(\tilde{\kappa}) > d(\tilde{\kappa}_1) \exp\left(\frac{d'(\tilde{\kappa}_1)}{d(\tilde{\kappa}_1)}(\tilde{\kappa} - \tilde{\kappa}_1)\right). \tag{27}$$

Proof. Recall first that $\tilde{\kappa} = K/|\Omega|$, so we may speak interchangeably of K and $\tilde{\kappa}$. It follows from Lemma 2.10 that D is positive on $[\tilde{\kappa}_1, \tilde{\kappa}_2]$, or equivalently

$$\frac{d''(\tilde{\kappa})}{d'(\tilde{\kappa})} < \frac{d'(\tilde{\kappa})}{d(\tilde{\kappa})}.$$

Integrating both sides from $\tilde{\kappa}_1$ to $\tilde{\kappa}$,

$$\log \frac{d'(\tilde{\kappa})}{d'(\tilde{\kappa}_1)} < \log \frac{d(\tilde{\kappa})}{d(\tilde{\kappa}_1)}$$
$$\frac{d'(\tilde{\kappa})}{d(\tilde{\kappa})} > \frac{d'(\tilde{\kappa}_1)}{d(\tilde{\kappa}_1)}.$$

Integrating again,

$$\log \frac{d(\tilde{\kappa})}{d(\tilde{\kappa}_1)} > \frac{d'(\tilde{\kappa}_1)}{d(\tilde{\kappa}_1)}(\tilde{\kappa} - \tilde{\kappa}_1),$$

which is (27). □

Proposition 2.9 is a corollary to Proposition 2.17.

We now present a final result limiting the instability of the system. Like Proposition 2.17, it establishes a lower bound for $d(\tilde{\kappa})$ in unstable regions based on local properties of d. It relies on a similar technique.

Proposition 2.18. *Given η, A_0, $\overline{B} > 0$ and a deterrence function d, let $[K_1, K_2]$ be an interval such that the system is linearly unstable if $K_1 \leq K \leq K_2$. Then there exist positive constants α_1, α_2, α_3, and p such that, if $K_1 < K \leq K_2$, then*

$$d(\tilde{\kappa}) > \alpha_1 + (\alpha_2 + \alpha_3(\tilde{\kappa} - \tilde{\kappa}_1))^{-p}. \tag{28}$$

Proof. By Lemma 2.10, if the system is linearly unstable, then

$$\frac{1}{3\overline{B}} \frac{d''(\tilde{\kappa})}{d'(\tilde{\kappa})} > -\frac{d'(\tilde{\kappa})}{(1 + \eta + d(\tilde{\kappa})\eta(d(\tilde{\kappa})\overline{B} + A_0))(d(\tilde{\kappa})\overline{B} + A_0) - 3\overline{B}d(\tilde{\kappa})}.$$

We would like to use the same procedure as in Proposition 2.17, integrating both sides to get a first-order differential inequality in d. However, the left-hand side is not integrable analytically, so we replace (20) with

$$1 + d(\tilde{\kappa})\eta\frac{A_0^2}{\tilde{A}} - 3D(\tilde{\kappa})\tilde{\rho} < -\eta, \tag{29}$$

which follows from (20) because $A_0 < \tilde{A}$. Write (29) as

$$3\overline{B}\frac{d'(\tilde{\kappa})^2}{d''(\tilde{\kappa})} < -(\eta A_0^2 + (\eta-2)\overline{B})d(\tilde{\kappa}) - (\eta+1)A_0. \tag{30}$$

The left-hand side is positive, so the right-hand side is also positive. Thus we may take reciprocals of both sides:

$$\frac{1}{3\overline{B}}\frac{d''(\tilde{\kappa})}{d'(\tilde{\kappa})^2} > \frac{1}{-(\eta A_0^2 + (\eta-2)\overline{B})d(\tilde{\kappa}) - (\eta+1)A_0}. \tag{31}$$

Let $b = -(\eta A_0^2 + (\eta-2)\overline{B})$, $c = (\eta+1)A_0$. By Proposition 2.12,

$$b > -\frac{2\overline{B}}{\overline{B}+A_0^2}A_0^2 - \left(\frac{2\overline{B}}{\overline{B}+A_0^2} - 2\right)\overline{B} = 0.$$

By (30), $bd(\tilde{\kappa}) - c > 0$. Write (31) as

$$\frac{1}{3\overline{B}}\frac{d''(\tilde{\kappa})}{d'(\tilde{\kappa})} < \frac{d'(\tilde{\kappa})}{bd(\tilde{\kappa}) - c} \tag{32}$$

Integrate (32) from $\tilde{\kappa}_1$ to $\tilde{\kappa}$:

$$\begin{aligned}
\frac{1}{3\overline{B}}\log\frac{d'(\tilde{\kappa})}{d'(\tilde{\kappa}_1)} &< \frac{1}{b}\log\frac{bd(\tilde{\kappa}) - c}{bd(\tilde{\kappa}_1) - c} \\
\frac{d'(\tilde{\kappa})}{d'(\tilde{\kappa}_1)} &< \left(\frac{bd(\tilde{\kappa}) - c}{bd(\tilde{\kappa}_1) - c}\right)^{3\overline{B}/b} \\
\frac{d'(\tilde{\kappa})}{(bd(\tilde{\kappa}) - c)^{3\overline{B}/b}} &> \frac{d'(\tilde{\kappa}_1)}{(bd(\tilde{\kappa}_1) - c)^{3\overline{B}/b}}.
\end{aligned} \tag{33}$$

Now observe

$$\begin{aligned}
-\eta A_0^2 - \eta\overline{B} &< \overline{B} \\
-\eta A_0^2 - (\eta-2)\overline{B} &< 3\overline{B} \\
b &< 3\overline{B}.
\end{aligned}$$

Thus $3\overline{B}/b > 1$, so integrating (33) gives

$$\frac{1}{b-3\overline{B}}\Big((bd(\tilde{\kappa}) - c)^{1-3\overline{B}/b} - (bd(\tilde{\kappa}_1) - c)^{1-3\overline{B}/b}\Big) > \frac{d'(\tilde{\kappa}_1)}{(bd(\tilde{\kappa}_1) - c)^{3\overline{B}/b}}(\tilde{\kappa} - \tilde{\kappa}_1)$$

Equivalently,

$$d(\tilde{\kappa}) > \frac{c}{b} + \frac{1}{b}\left((c - bd(\tilde{\kappa}_1))^{1-3\overline{B}/b} + \frac{(b-3\overline{B})d'(\tilde{\kappa}_1)}{(c - bd(\tilde{\kappa}_1))^{3\overline{B}/b}}(\tilde{\kappa} - \tilde{\kappa}_1)\right)^{b/(b-3\overline{B})}.$$

Bringing $1/b$ inside the parentheses yields (28). □

Corollary 2.19. *If $K \geq d^{-1}(c/b)|\Omega|$, then the system is linearly stable.*

3. **Numerical implementation.** First we describe our procedure for solving (8-9) numerically. Divide the two-dimensional torus Ω into an equally spaced square grid with N nodes on each side, distance h apart. Fixed time steps suffice. Let (A^n, ρ^n, κ^n) denote the state of the system at time step n.

To calculate A^{n+1} and ρ^{n+1} from (A^n, ρ^n, κ^n), we use a finite difference scheme closely resembling the one described in [19]. However, rather than tracking the criminal density ρ at each step, we track an attractiveness-normalized criminal density $z = \rho/A$. Equations (8-9) become

$$\frac{\partial A}{\partial t} = \eta \triangle A + d(\kappa) A^2 z - (A - A_0) \tag{34}$$

$$\frac{\partial z}{\partial t} = \triangle z - \left(\frac{(1+\eta)\triangle A - (A - A_0)}{A} - d(\kappa) A \right) z - d(\kappa) A z^2 + d(\kappa) \frac{\overline{A} - A_0}{A}. \tag{35}$$

As Sun [22] observes, this transformation banishes the advective term in (9), eliminating concerns about upwinding. Equations (34-35) are solved numerically by a semi-implicit method, using spectral methods for the implicit part, following [19].

In the following we outline the procedure for solving the optimization problem, which in the discrete context is to find $\kappa^{n+1} \in \mathbb{R}^{N \times N}$ solving

$$\kappa^{n+1} = \arg\min \left\{ \sum_{i,j=1}^{N} d(k_{i,j}) \rho_{i,j}^{n+1} A_{i,j}^{n+1} : k_{i,j} \geq 0, \sum_{i,j=1}^{N} k_{i,j} = K \right\}.$$

Efficiency will be important, as the optimization problem must be solved anew in every time step. The strategy will be to reduce the problem to solving a nonlinear equation in a single (integer) variable and then using a combination of iterative methods to solve this equation. When $d(k) = e^{-k}$, the form of the nonlinear equation will suggest a simpler algorithm.

3.1. **Reduction of the problem.** We can reduce this problem to solving a nonlinear equation, reminiscent of section 2.2 above. We are given two-dimensional vectors ρ^{n+1} and A^{n+1} and seek κ^{n+1}.

Rearrange the N^2 values of $\rho_{i,j}^{n+1} A_{i,j}^{n+1}$ into a one-dimensional vector $f \in \mathbb{R}^{N^2}$, so that its values are in descending order. If α is the coordinate map mediating the two ($f_{\alpha(i,j)} = \rho_{i,j}^{n+1} A_{i,j}^{n+1}$), then it is natural to define another vector $\xi \in \mathbb{R}^{N^2}$ by $\xi_{\alpha(i,j)} = \kappa_{i,j}^{n+1}$; that is, ξ is the rearrangement of κ^{n+1} matching the rearrangement of f. We can recast the optimization problem in terms of ξ: we want to find $\xi \in \mathbb{R}^{N^2}$ minimizing $\sum_{\alpha=1}^{N^2} d(\xi_\alpha) f_\alpha$ subject to $\xi_\alpha \geq 0$, $\sum_{\alpha=1}^{N^2} \xi_\alpha = K$.

In the optimal configuration there will be a β such that $\xi_\alpha > 0$ if $\alpha < \beta$ and $\xi_\alpha = 0$ if $\alpha > \beta$. Any police deployed to the right of such a β would be more effective deployed to the left of β. If β is known, we can restrict consideration to the dimensions in which ξ is positive. A straightforward application of Lagrange multipliers then gives that $d'(\xi_\alpha) f_\alpha$ must be the same for all α between 1 and β. We can use this to read off the values of ξ:

$$\xi_\alpha = \begin{cases} (d')^{-1}(d'(0) f_\beta / f_\alpha) & \text{if } \alpha \leq \beta, \\ 0 & \text{otherwise.} \end{cases} \tag{36}$$

Determining ξ is thus a matter only of solving the nonlinear resource constraint equation for β:

$$G(\beta) := \sum_{\alpha=1}^{\beta} (d')^{-1}\left(d'(0)\frac{f_\beta}{f_\alpha}\right) = K. \tag{37}$$

We can then recover κ^{n+1} if we know the coordinate map $\alpha(i,j)$. The above equation has at most one solution, because G is increasing:

$$G(\beta+1) - G(\beta) = (d')^{-1}\left(d'(0)\frac{f_{\beta+1}}{f_{\beta+1}}\right) + \sum_{\alpha=1}^{\beta}\left((d')^{-1}\left(d'(0)\frac{f_{\beta+1}}{f_\alpha}\right) - (d')^{-1}\left(d'(0)\frac{f_\beta}{f_\alpha}\right)\right)$$

The extra $\beta+1$ term is 0. By construction f is decreasing, and $(d')^{-1}$ is increasing because d' is. Thus $G(\beta+1) - G(\beta) > 0$.

It is of course unlikely that we will find a β solving (37) exactly. Rather, there will be some β for which $G(\beta) < K$ but $G(\beta+1) > K$. If we then set ξ as in (36), there will be some police left over, which for convenience we will distribute evenly among those ξ_α for which $\alpha \le \beta$. We do not expect this small liberty we've taken to affect the results meaningfully.

As we noted above, to use this reduction we need to determine $\alpha(i,j)$. The first time we do this we can expect it to take $O(N^2 \log N)$ floating point operations using the quicksort algorithm on f. However, if the time step is small, α should not change very much between time steps. Thus if we use the previous time step's α as an initial guess we can expect quicksort to finish in less than $O(N^2 \log N)$.

It may be that K is so large that (37) has no solution for $\beta \le N^2$. In this scenario the police will deploy to every grid point. It is still the case that $d'(\xi_\alpha)f_\alpha$ is the same for all α; in fact, they equal λ, the Lagrange multiplier of the ℓ^1 constraint. The problem in this case is to solve

$$H(\lambda) := \sum_{\alpha=1}^{N^2} (d')^{-1}(-\lambda/f_\alpha) = K$$

for λ; then $\xi_\alpha = (d')^{-1}(-\lambda/f_\alpha)$. This is a problem in a continuous variable, and standard iterative methods suffice. They are unfortunately expensive because we have to sum all the way to N^2 at each iteration. For the following we restrict consideration to the harder scenario in which $\beta < N^2$.

3.2. **General deterrence: a discrete false position method.** We now present the iterative method to solve (37). Our main workhorse will be the false position method, but we will use the secant method to initialize a window of an appropriate size and bisection if the false position method stalls, as it can near the solution.

We begin with an initial guess β^0. Suppose $G(\beta^0) < K$; then we know $\beta \in [a^0, b^0]$, where $a^0 = \beta$ and $b = N^2$. If β^0 is a good initial guess, then information around β^0 will be more helpful than information around N^2. Therefore, we hold off on beginning false position at first. We compute β^1 using the secant method, with $G(\beta^0+1) - G(\beta^0)$ as the slope. If $G(\beta^1) > K$, we let $a^1 = a^0$, $b^1 = \beta^1$, and switch to the false position method. Otherwise, we let $a^1 = \beta^1$, $b^1 = b^0$, and repeat until $G(\beta^n) > K$. The same method works *mutatis mutandis* for when $G(\beta^0) > K$; in this case we repeat until $G(\beta^n) < K$, when we set $a^n = \beta^n$.

Once we have $b^n < N^2$, we use a discrete false position method to narrow the window $[a^n, b^n]$ progressively. The false position method applied to a discrete function can stall as the window narrows to the solution; that is, it can select $[a^{n+1}, b^{n+1}] = [a^n, b^n]$. In practice we found this happened a significant minority of the time. In these cases we switched to bisection to guarantee convergence.

We have no reason to expect to guess β close to correctly *a priori*, so we can expect this algorithm to be expensive the first time it is run in any given simulation. However, we do not expect β to change much between successive time steps, so using the prior time step's solution as an initial guess should speed up successive runs of the algorithm.

3.3. **Exponential deterrence: a homomorphism-based method.** When $d(k) = e^{-k}$, G has the form

$$G(\beta) = \sum_{\alpha=1}^{\beta} \log(f_\alpha / f_\beta).$$

Computing $G(\beta)$ directly requires β logarithm evaluations, so we would prefer to evaluate it as few times as possible. In fact we can cut down the work significantly by observing the following consequence of the fact that the logarithm is a homomorphism:

$$G(\beta) = G(\beta - 1) + \beta \log \frac{f_{\beta-1}}{f_\beta}. \tag{38}$$

This means that starting by calculating $G(1)$ and incrementing until $G(\beta) \geq K$ takes about β logarithm evaluations and 3β additional floating point operations, a very reasonable cost. We therefore simply compute $G(\alpha)$ recursively until we find $G(\alpha) > K$, and set $\beta = \alpha - 1$.

4. **Numerical results.** We present several results from runs of the finite difference scheme. First we present several solution patterns and discuss them qualitatively. Then we consider patterns of police distribution for different values of K, the total amount of police. Finally we return to Proposition 2.8 and consider the relationship between K and ϵ, the amplitude of a Fourier perturbation off the homogeneous steady state.

4.1. **Solution behavior.** We present the results of several runs of the numerics described in the previous sections. In each case we used grid size $N = 256$, grid spacing $dx = \frac{1}{4}$, and periodic boundary conditions. The length of the time step varied between 0.02 and 0.5 depending on observed stability criteria.

We observed three regimes of behavior, illustrated in Fig. 3. In general, hotspots respond to the introduction of police by expanding in radius but decreasing in height. When there are few police, the hotspots widen slightly and then remain at equilibrium (Fig. 3b). When there are many police, the hotspots all overlap, and the system approaches a spatially homogeneous equilibrium (Fig. 3d). These states correspond to the two kinds of equilibrium states observed in the model without police, namely hotspots and no hotspots. However, a moderate number of police can produce an intermediate state in which hotspots merge only with a few neighbors, creating a system of persistent "warm worms" with a diffuse interface into worm-like cold regions of little crime (Fig. 3c). In this case the police and criminals both remain within the warm regions. We have observed this behavior with several choices of deterrence function d.

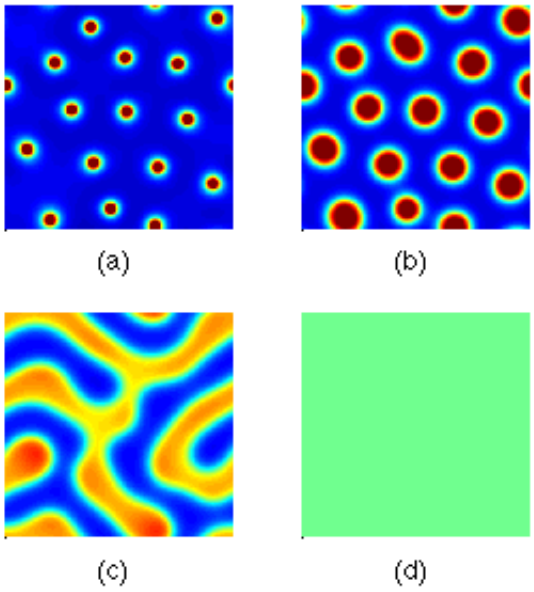

FIGURE 3. Plots of the criminal density ρ from numerical solutions of (8-10). Here $d(k) = e^{-k}$. (a) A near-steady-state solution with $\eta = 0.03$, $A_0 = 0.5$, $\overline{B} = 2.5$, and no police, same as Fig. 2. (b) The same system at time 500 after $K = 300$ police were introduced at time 0. (c) $K = 500$, $t = 500$. (d) $K = 700$, $t = 500$.

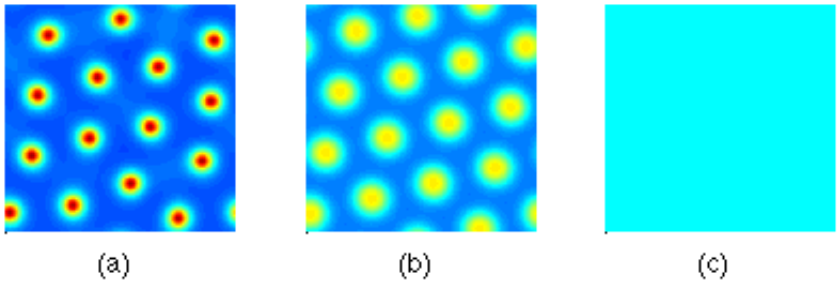

FIGURE 4. Plots of the criminal density ρ from numerical solutions of (8-10) Here $d(k) = e^{-k}$. (a) A near-steady-state solution with $\eta = 0.05$, $A_0 = 1.1$, $\overline{B} = 2.9$, and no police. (b) The same system at time 500 after $K = 0.66$ police were introduced at time 0. (c) $K = 0.67$, $t = 500$.

The third regime is absent under some parameter choices. Fig. 4 shows two plots of a system with two close values of K ($K = 0.66$ for (b) and $K = 0.67$ for (c)). One produces hotspot flattening and the other hotspot dissipation, with no apparent intermediate regime of warm worms. Fig. 4 suggests a geometric explanation: the

hotspots are distributed so uniformly (compare with Fig. 3) that a hotspot cannot collide with one neighbor without colliding with them all.

Qualitatively, the "warm worms" solution resembles well known phase-separated solutions of the Cahn-Hilliard equation [6]. In that case, the phase separation arises from the double-well Ginzburg-Landau potential. In our equations, however, the only equilibrium, stable or otherwise, is given by (16). Moreover, the values of A, ρ, and κ at the worms' peaks are greater than the equilibrium values, and the values at the troughs are less. The dynamics here are clearly quite different from the Cahn-Hilliard dynamics.

The "warm worms" regime does not appear stable; indeed, once the topology settles we observe a slow drift in the system, in the worms' prevailing direction. It is possible that the worms regime is a metastable state that in the long run will approach either the first or third regime (that is, flattened hot spots or homogeneous equilibrium). This convergence has not occurred on the time scales we have considered.

4.2. **Dynamics of κ.** The three regimes are also reflected in Fig. 5. Here our initial condition resembles Fig. 2, a state of stable hotspots found by running the original Short model. At $t = 0$ we introduce police and run until $t = 1000$, varying the value of K between runs. We then plotted the maximum value of κ in each simulation against K, yielding the solid line. We repeated this process starting from a homogeneous initial condition, as well; this is the dashed line.

The hotspot flattening regime ends at about $K = 420$, when $\max \kappa$ abruptly turns downward. The warm worms regime ends at around $K = 580$, when we get total hotspot suppression and the two branches merge. The bumpy pattern in the intermediate regime is consistent with the notion that warm worms is not a stable regime. Sudden changes in $\max \kappa$ occur at transition points in the topology of the worms, as shown in the inset images.

We have not plotted $\min \kappa$ as part of Fig. 5. For the dashed line minimum and maximum coincide, while for the solid line the minimum is 0 until the branches merge, at which point it joins them. In all our simulations, if $\min \kappa$ ever exceeds 0 the system ultimately converges to homogeneous equilibrium.

4.3. **Return to linear stability.** We now investigate Proposition 2.8 numerically. For a given value of K, consider the initial condition $A(x, 0) = \tilde{A} + \epsilon f(x)$, $\rho(x, 0) = \tilde{\rho} + \epsilon f(x)$, where ϵ is a small positive parameter, f is a Fourier perturbation, and $\tilde{A}$ and $\tilde{\rho}$ are the homogeneous equilibrium values of A and ρ for the given parameters, including K, given in (16). Proposition 2.8 tells us that, for a small enough value of ϵ, κ will be nonzero everywhere. The only steady states we have observed in which the police deploy everywhere is the homogeneous steady state; that is, in all observed cases where κ is eventually supported throughout Ω, (A, ρ) converges to $(\tilde{A}, \tilde{\rho})$.

We can ask then, given K, what critical value of ϵ separates the regimes where the system converges to $(\tilde{A}, \tilde{\rho})$ or remains spatially heterogeneous. Fig. 6 shows this critical value $\epsilon^*(K)$ for several values of K. We found this value numerically, by doing a binary search through different candidate values and then running the scheme described above. The relationship between K and $\epsilon^*(K)$ appears linear.

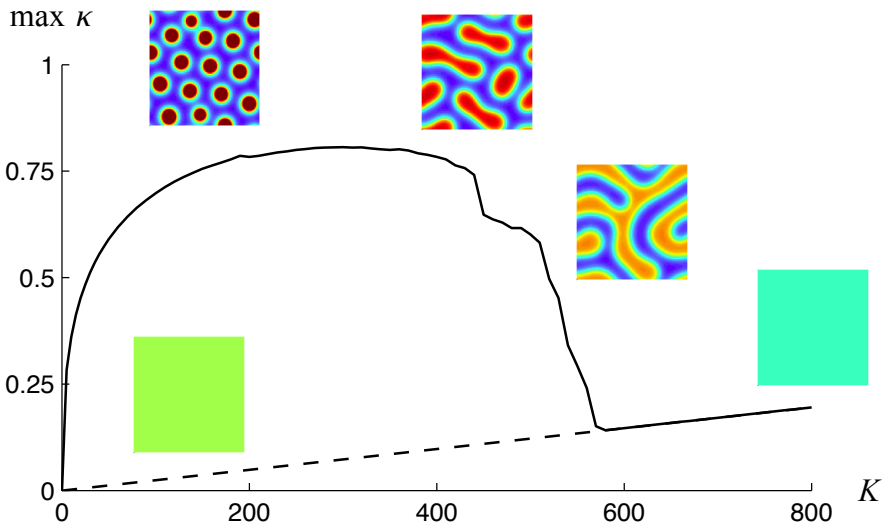

FIGURE 5. Data gathered from solutions of (8-10) with $\eta = 0.03$, $A_0 = 0.5$, $\overline{B} = 2.5$. For different values of K, the maximum value of κ at time $t = 1000$ is plotted for two classes of solutions. The solid line comes from solutions seeded with an initial condition of stable hot spots. The dashed line comes from solutions seeded with the homogeneous equilibrium values (16). Inset pictures are snapshots of A.

4.4. **Comparison with the discrete model.** We now implement police within the discrete, stochastic crime model introduced in [19] and described briefly in section 1.2. As in the continuous model, police should decrease the rate at which new criminals enter the system and discourage existing criminals from committing crimes. The former effect is accomplished by replacing the constant criminal birth parameter Γ in (3) with the spatially varying $d(\kappa(x,t))\Gamma$. The latter effect is accomplished modifying the strike probability specified in (1):

$$p_s(x,t) = 1 - e^{-d(\kappa(x,t))A(x,t)dt}.$$

All that remains is the rule for choosing κ. In the discrete model there is no continuous criminal density ρ, only the integer-valued number of criminals n. Using nA in the place of ρA in the objective function for κ produces a discontinuous κ whose support is highly irregular. It also implies that the police know where every criminal is at any given time, rather than the overall distribution of criminals represented by ρ. Instead we use A^2, which like ρA is steeper than A but follows its pattern of high and low values. At time t κ is chosen by

$$\kappa = \arg\min \left\{ \sum_{i,j=1}^{N} d(k_{i,j}) A_{i,j}(t)^2 : k \in \mathbb{R}^{N\times N}, k_{i,j} \geq 0, \sum_{i,j=1}^{N} k_{i,j} = K \right\}.$$

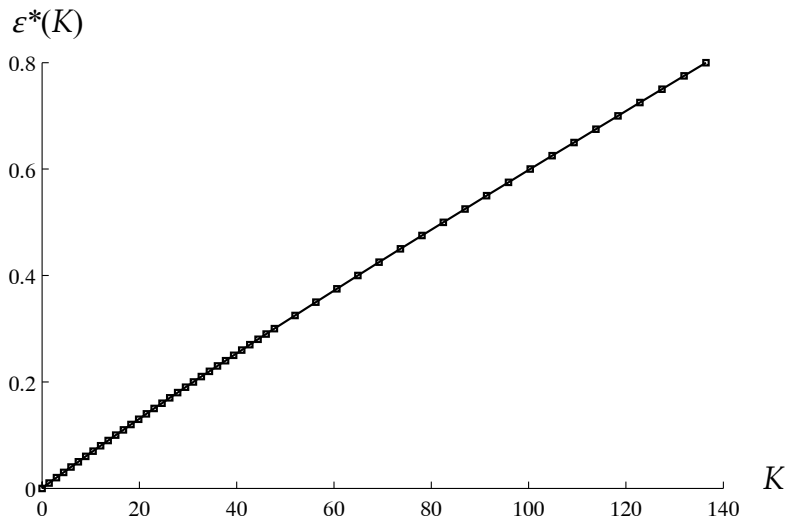

FIGURE 6. Given police resources K, $\epsilon^*(K)$ is the critical amplitude of the Fourier perturbation in an initial condition for (8-10). For values of ϵ below $\epsilon^*(K)$, the system converges to homogeneous equilibrium. For values of ϵ above $\epsilon^*(K)$, the system remains spatially heterogeneous.

The algorithms described in section 3 can be used here, with $f = A^2$ instead of $f = \rho A$.

Fig. 7 shows snapshots of the attractiveness A from numerical simulations of the discrete model with police. We begin with (a), a state with stationary hot spots. Then in (b), (c), and (d) we add 300, 500, and 700 police, respectively, and let time run, as in Fig. 3. We see several characteristics shared with the continuous system as shown in Fig. 3. In particular, (c) shows a "warm worms" regime arising in the discrete model, as well. The worms evolve differently than in the continuous system because of the discrete system's stochastic nature.

5. **The radial problem for small police forces.** The first behavior regime (flattened hot spots) is represented in Fig. 5 to the left of $K \approx 400$. For small K the police are concentrated entirely within the hot spot centers, and the increase in $\max \kappa$ is faster than $K^{1/2}$. To better understand this small-K behavior we focus on the case of a single hotspot in steady state when total police resources K is small. For simplicity we take $d(k) = e^{-k}$ for this section. As in [15], replace ρ with the transformed variable $V = \rho/A^2$ to simplify the ODEs. Now $d(\kappa)VA^3$ represents the total crime at a location.

5.1. **Restatement as a boundary-value problem.** The governing equations are radially symmetric, so any such solution should be radially symmetric. Changing the spatial coordinates to radial and assuming a steady state, we have the ODE

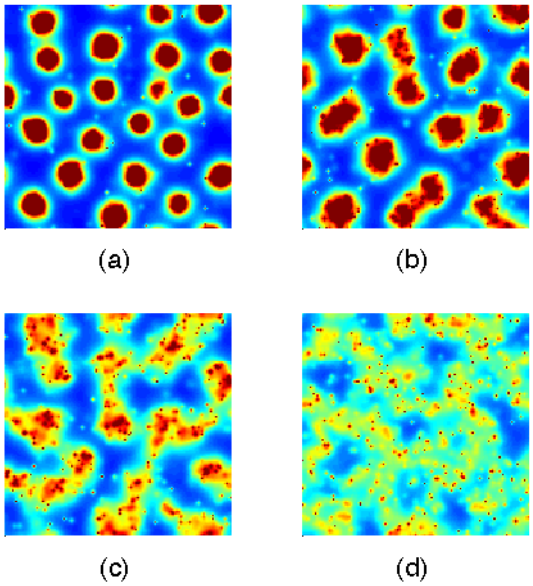

FIGURE 7. Plots of the attractiveness A from numerical solutions of the discrete system with police. In all cases $A_0 = \frac{1}{30}$, $\eta = 0.03$, $\omega = \frac{1}{15}$, $\theta = 0.56$, $\Gamma = 0.02$, $d(k) = e^{-k}$. (a) Stationary hot spots without police (b) The same system at time 400 after $K = 300$ police were introduced at time 0. (c) $K = 500$, $t = 400$. (d) $K = 700$, $t = 400$.

system

$$\begin{aligned} 0 &= (rA_r)_r + d(\kappa)VA^3 - A + A_0 \\ 0 &= (rV_rA^2)_r - d(\kappa)VA^3 + d(\kappa)\overline{B} \\ \kappa &= (d')^{-1}(-\lambda/\rho A)\chi_{U(\lambda,\rho A)} \end{aligned}$$

where $\lambda > 0$ satisfies

$$\int_{U(\lambda,\rho A)} (d')^{-1}(-\lambda/\rho A) r\, dr = K.$$

K can be rescaled by 2π without loss of generality.

The notion is that we have a hotspot centered at the origin, so total crime should be decreasing in r until it reaches a trough, say at $r = \beta$, whose value would in the full two-dimensional system be determined by the proximity of other hot spots. Because VA^3 is decreasing and K is small, we can predict that $U(\lambda, \rho A)$ will be an interval with one endpoint at the origin and the other endpoint at some $b \in (0, \beta)$. Furthermore, we can take advantage of Corollary 2.7 to simplify $d(\kappa)VA^3 =$

$V(b)A(b)^3$ within $(0,b)$. We therefore have a boundary-value problem:

$$0 = \tfrac{\eta}{r}(rA_r)_r + V(b)A(b)^3 - A + A_0 \qquad \text{if } 0 < r < b, \tag{39}$$

$$0 = \tfrac{1}{r}(rV_rA^2)_r - V(b)A(b)^3 + \overline{B}\tfrac{V(b)A(b)^3}{VA^3} \qquad \text{if } 0 < r < b, \tag{40}$$

$$0 = \tfrac{\eta}{r}(rA_r)_r + VA^3 - A + A_0 \qquad \text{if } b < r < \beta, \tag{41}$$

$$0 = \tfrac{1}{r}(rV_rA^2)_r - VA^3 + \overline{B} \qquad \text{if } b < r < \beta, \tag{42}$$

$$K = \int_0^b \log\left(\frac{VA^3}{V(b)A(b)^3}\right) r\,dr \tag{43}$$

The boundary conditions are $A'(0) = V'(0) = A'(\beta) = V'(\beta) = 0$ and A and V continuous across b. We have also specified that the hotspot peaks at 0 and troughs at β.

Next we show that regular solutions to this boundary-value problem are regular at the boundary. First note that a simple analog to Theorem 2.2 holds for this radial problem, by parallel reasoning.

Proposition 5.1. *Any solution (V, A) to the boundary-value problem that is C^2 in $(0,b)$ and C^2 in (b,β) is C^2 in $(0,\beta)$.*

Proof: It suffices to show that V and A are C^2 across b. It is given that V and A are continuous across b. Furthermore, because $d(\kappa)$ is a continuous function of r by Proposition 2.2, $d(\kappa)VA^3 - A + A_0$ is a continuous function of r. Thus $\frac{\eta}{r}(rA_r)_r$ is continuous through b, and hence so is $(rA_r)_r$. This means that the antiderivative rA_r is C^1 around b, and hence A_r is C^1 at b. Thus A is C^2 around b.

Likewise, $-d(\kappa)VA^3 + d(\kappa)\overline{B}$ is continuous at b, so $(rV_rA^2)_r$ is. Thus V_rA^2 is C^1. We just showed A is C^2, so V_r is C^1. Thus V is C^2.

In particular, Proposition 5.1 allows us to use a similar numerical scheme to that used on the full 2D problem without treating the boundary specially. We outline the numerical method in the next section.

We conclude by noting briefly that (39) has a general solution in terms of a Bessel function of the first kind, namely

$$A(r) = A_0 + V(b)A(b)^3 + (A(0) - A_0 - V(b)A(b)^3)J_0(ir/\sqrt{\eta}).$$

Taylor coefficients for a series solution for V in $(0,b)$ can be derived from (39) and (40).

5.2. **Numerical method.** We compute solutions to (39-43) by running a fixed-point iteration, essentially simulating the time-dependent equations until they reach steady state. At each step we must solve a finite difference problem and an optimization problem. Our initial condition is a low trough away from the origin and a peak at the origin, so that with the right choice of parameters the steady state will be a hot spot centered at the origin.

The finite difference solver is based on the same transformation (34-35) used in the 2D problem. The only extra difficulty is the degeneracy of the radial Laplacian at the origin. Here we employ standard techniques for dealing with degenerate diffusion, following [24]. If our domain is partitioned into a grid by $0 = r_0 < r_1 < r_2 < \cdots < r_N = \beta$, then the discrete Laplacian operator $\triangle_r$ is defined by

$$(\triangle_r u)_i = \frac{2}{r_{i+1}^2 - r_i^2}\left(\frac{2r_{i+1}}{r_{i+2} - r_i}(u_{i+1} - u_i) - \frac{2r_i}{r_{i+1} - r_{i-1}}(u_i - u_{i-1})\right)$$

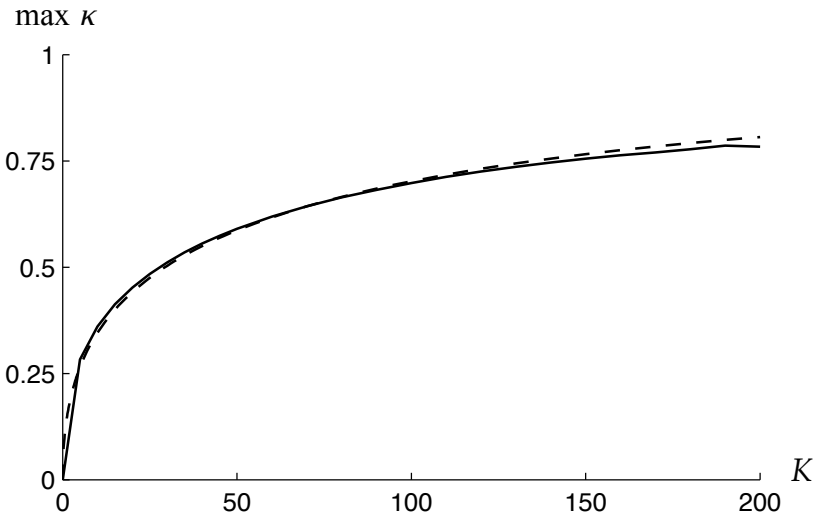

FIGURE 8. $\max \kappa(\cdot, t)$ vs. K at $t = 500$ for the two-dimensional problem (solid) and the radial problem (dashed).

for $1 \le i \le N-2$. With Neumann boundary conditions the edge terms are

$$(\triangle_r u)_0 = \frac{8}{r_1 r_2}(u_1 - u_0),$$
$$(\triangle_r u)_{N-1} = -\frac{2}{r_N^2 - r_{N-1}^2}\frac{2r_{N-1}}{r_N - r_{N-2}}2(u_{N-1} - u_{N-2}).$$

Offsetting the extra difficulty of implementing degenerate diffusion, the above operator $\triangle_r$ is tridiagonal, so the implicit part of each finite difference step can be solved in $O(N)$ time. Also, it can be defined on grids of variable length.

The optimization solver is essentially the same as in the 2D exponential case, relying on the identity (38). The radial solver is actually simpler because total crime is decreasing on $(0, \beta)$, and therefore we needn't sort the grid points every time step.

Because we plan to investigate the problem for small values of K, we choose the grid to be fine near the origin and coarser away from the origin. This will give us a more precise κ contour.

5.3. **Results.** Fig. 8 shows that the radial problem reproduces the small-K behavior of the full 2-D problem. The solid line is the same as in Fig. 5, while the dashed line shows results from the radial simulation. The shapes are nearly identical for small K. They settle to lines of different slope for large K only because their domains are different. The radial problem's transition between steady states occurs at about $K = 550$, when the two-dimensional problem is still in the "warm worms" regime. This may suggest that the warm worms are indeed a metastable state connecting two stable equilibria (flattened hot spots and homogeneity).

6. **Conclusion.** We have introduce into the Short model police behavior that seeks to minimize crime. The equations can be restated as a free-boundary problem, with the boundary being a level set of the crime level ρA determined by λ, the dual variable associated to the L^1 constraint on police resources. Given enough police, the linear instability in the original Short model is stabilized. We present a numerical scheme and discuss patterns in the results.

Several of our results suggest that even a temporary infusion of police into a crime-ridden area can reduce crime. In section 4 we provided sudden infusions of police to an area with existing hot spots of crime. For the initial condition considered in Fig. 5, when K was greater than about 650 the hot spots were wiped away completely by $t = 500$. However, the case of Fig. 3(c) is instructive: if there are not enough police, the effect can be to reduce crime overall but greatly increase the area over which criminals act. This recalls the discrete version of the original Short model, which in some parameter regimes had migratory hot spots. This may be an undesirable result for policymakers. Even if the "warm worms" regime is a metastable transition state toward homogeneous equilibrium, the transition would occur over a timescale that policymakers may find unacceptable.

Indeed, the status of the "warm worms" regime remains an open problem. An investigation of the bifurcation theory of the two stable states may provide some clues. Another open problem is the well posedness of the free-boundary problem (8-12). We saw that police generally stabilize the hot spots, but regularity may be lost across the free boundary. If a two-dimensional analogue to Proposition 5.1 holds, then there is at least some regularity. Sharper results on the linear stability of the two-dimensional system would also be welcome.

Several extensions of this work also present themselves. We assume here that police react instantaneously to changes in the total crime ρA. In practice they receive delayed, incomplete, noisy indicators of the amount of crime. Even with improved information, police officials generally make decisions at regularly scheduled meetings rather than continuously. One possible way to model this would be to force κ to be piecewise constant in time, only changing at certain prescribed values of t, and to force police to optimize against an outdated picture of ρA.

Though police presence in (8-12) modifies criminal perception and behavior to some extent, the core of their dynamics still arises from the random walk model described in section 1.2. Routine activity theory suggests that criminals are not as strategic as police, but it also suggests that they are at least somewhat strategic as they evaluate their opportunities. A more complete treatment would consider the interplay between criminal and police strategies using the tools of game theory.

Acknowledgments. The first author thanks Jeffrey Brantingham, Christoph Brune, and Theodore Kolokolnikov for helpful discussions.

REFERENCES

[1] H. Berestycki and J.-P. Nadal, *Self-organised critical hot spots of criminal activity*, Eur. J. Appl. Math., **21** (2010), 371–399.

[2] H. Berestycki, N. Rodríguez and L. Ryzhik, *Traveling wave solutions in a reaction-diffusion model for criminal activity*, arXiv:1302.4333

[3] Daniel Birks, Michael Townsley and Anna Stewart, *Generative explanations of crime: using simulation to test criminological theory*, Criminology, **50** (2010), 221–254.

[4] Anthony A. Braga, *The effects of hot spots policing on crime*, Ann. Am. Acad. Polit. S. S., **578** (2001), 104–125.

[5] Paul J. Brantingham and Patricia L. Brantingham, "Patterns in Crime,", Macmillan, 1984.

[6] John W. Cahn and John E. Hilliard, *Free energy of a nonuniform system. I. Interfacial free energy*, J. Chem. Phys., **28** (1958), 258–67.
[7] Robert S. Cantrell, Chris Cosner and Raúl Manásevich, *Global bifurcation of solutions for crime modeling equations*, Siam J. Math. Anal., **44** (2012), 1340–1358.
[8] Sorathan Chaturapruek, Jonah Breslau, Daniel Yazdi, Theodore Kolokolnikov and Scott G. McCalla. *Crime modeling with Lévy flights*, Siam J. Appl. Math., **73** (2013), 1703–1720.
[9] John E. Eck and David Weisburd, *Crime places in crime theory*, in "Crime and Place: Crime Prevention Studies" (eds. John E. Eck and David Weisburd), Criminal Justice Press, (1995), 1–33.
[10] T. Hillen and K. J. Painter, *A user's guide to PDE models for chemotaxis*, J. Math. Biol., **58** (2009), 183–217.
[11] S. D. Johnson, K. Bowers and A. Hirschfield, *New insights into the spatial and temporal distribution of repeat victimization*, British J. Criminol, **37** (1997), 224–241.
[12] Paul A. Jones, P. Jeffrey Brantingham and Lincoln R. Chayes, *Statistical models of criminal behavior: the effects of law enforcement actions*, Math. Mod. Meth. Appl. S., **20** (2010), 1397–1423.
[13] Evelyn F. Keller and Lee A. Segel, *Initiation of slime mold aggregation viewed as an instability*, J. Theor. Biol., **26** (1970), 399–415.
[14] Evelyn F. Keller and Lee A. Segel, *Model for chemotaxis*, J. Theor. Biol., **30** (1970), 225–234.
[15] T. Kolokolnikov, M. J. Ward and J. Wei, *The stability of steady-state hot-spot patterns for a reaction-diffusion model of urban crime*, to appear in Discrete Cont. Dyn.-B, arXiv:1201.3090.
[16] Ashley B. Pitcher, *Adding police to a mathematical model of burglary*, Eur. J. Appl. Math., **21** (2010), 401–419.
[17] Nancy Rodríguez, *On the global well-posedness theory for a class of PDE models for criminal activity*, Physica D, **260** (2013), 191–200.
[18] Nancy Rodríguez and Andrea Bertozzi, *Local existence and uniqueness of solutions to a PDE model for criminal behavior*, Math. Mod. Meth. Appl. S., **20** (2010), 1425–1457.
[19] M. B. Short, M. R. D'Orsogna, V. B. Pasour, G. E. Tita, P. J. Brantingham, A. L. Bertozzi and L. B. Chayes, *A statistical model of criminal behavior*, Math. Mod. Meth. Appl. S., **18** (2008), 1249–1267.
[20] M. B. Short, A. L. Bertozzi and P. J. Brantingham, *Nonlinear patterns in urban crime: hotspots, bifurcations, and suppression*, SIAM J. Appl. Dyn. Syst., **9** (2010), 462–483.
[21] Martin B. Short, P. Jeffrey Brantingham, Andrea L. Bertozzi and George E. Tita, *Dissipation and displacement of hotspots in reaction-diffusion models of crime*, P. Natl. Acad. Sci. USA, **107** (2010), 3961–3965.
[22] Hui Sun, *Continuum equations for crime modeling with random process*, unpublished report, UCLA (2010).
[23] Michael Townsley, Shane D. Johnson and Jerry H. Ratcliffe, *Space time dynamics of insurgent activity in Iraq*, Security J., **21** (2008), 139–146.
[24] Yao Yao and Andrea L. Bertozzi, *Blow-up dynamics for the aggregation equation with degenerate diffusion*, Physica D, **260** (2013), 77–89.

Received xxxx 20xx; revised xxxx 20xx.

E-mail address: jzipkin@math.ucla.edu
E-mail address: mbshort@math.gatech.edu
E-mail address: bertozzi@math.ucla.edu